Solar Cells

Deutsche Ausgabe: DOI: 10.1002/ange.201604307
Internationale Ausgabe: DOI: 10.1002/anie.201604307

# Thieno[3,4-*c*]pyrrole-4,6-dione-3,4-difluorothiophene Polymer Acceptors for Efficient All-Polymer Bulk Heterojunction Solar Cells

*Shengjian Liu[+], Zhipeng Kan[+], Simil Thomas, Federico Cruciani, Jean-Luc Brédas, and Pierre M. Beaujuge**

***Abstract:*** *Branched-alkyl-substituted poly(thieno[3,4-c]pyrrole-4,6-dione-alt-3,4-difluorothiophene) (PTPD[2F]T) can be used as a polymer acceptor in bulk heterojunction (BHJ) solar cells with a low-band-gap polymer donor (PCE10) commonly used with fullerenes. The "all-polymer" BHJ devices made with PTPD[2F]T achieve efficiencies of up to 4.4 %. While, to date, most efficient polymer acceptors are based on perylenediimide or naphthalenediimide motifs, our study of PTPD[2F]T polymers shows that linear, all-thiophene systems with adequately substituted main chains can also be conducive to efficient BHJ solar cells with polymer donors.*

"All-polymer" bulk heterojunction (BHJ) solar cells, consisting of a π-conjugated polymer donor intimately mixed with a polymer acceptor, which is used as an alternative to fullerenes (e.g. $PC_{61}BM$, or its $C_{71}$ analogue), have initially met with limited power conversion efficiencies (PCEs).[1] In these systems, concurrently achieving the appropriate phase-separated pattern and adequate charge transfer between donor and acceptor components can be challenging and, to date, only a few polymer acceptors have been shown to yield BHJ device PCEs greater than 3 %.[2] In comparison, BHJ solar cells composed of polymer donors and fullerenes can achieve PCEs of greater than 11 %,[3] although the lack of morphological stability and mechanical conformability of fullerene-based BHJ solar cells remains a matter of examination.[4] At this time, most efficient polymer acceptors are based on perylenediimide (PDI)[5] or naphthalenediimide (NDI) motifs,[4,6] and a few recent studies have shown that PDI/NDI-based analogues can achieve PCEs greater than 5 % with selected polymer donors.[4–6] A number of promising alternative acceptor motifs have been proposed, such as diketopyrrolopyrrole,[7] benzothiadiazole,[8] isoindigo,[9] B←N bridged thienylthiazole,[10] and various nitrile-derived motifs,[1,11] with reported PCEs in range of 1–5 %. However, the manifold of polymer acceptors which are rivaling fullerenes in BHJ solar cells remains modest, and broadening the class of polymer acceptors for further examination of the all-polymer BHJ concept is a critically important step in gradually improving device performance beyond currently reported PCEs.

Nonfullerene acceptors, including polymers, have important practical implications which span synthetic accessibility and potentially low synthetic costs compared to those incurred by the synthesis and extensive purifications of fullerene analogues.[2,12] In this contribution, we report on a set of branched-alkyl-substituted polymer acceptors composed of thieno[3,4-*c*]pyrrole-4,6-dione (TPD)[13] and 3,4-difluorothiophene ([2F]T)[14] motifs, and show that the appropriately functionalized all-thiophene analogue poly(thieno[3,4-*c*]pyrrole-4,6-dione-*alt*-3,4-difluorothiophene), namely PTPD[2F]T (Figure 1 a), can achieve PCEs of up to 4.4 % in BHJ solar cells with PCE10 (poly[4,8-bis(5-(2-ethylhexyl)thiophen-2-yl)benzo[1,2-*b*;4,5-*b*′]dithiophene-2,6-diyl-*alt*-(4-(2-ethylhexyl)-3-fluorothieno[3,4-*b*]thiophene-)-2-carboxylate-2–6-diyl)], also commonly referred to as PTB7-Th) as the polymer donor (model system; Figure 1 b). The donor ($E_{opt} \approx 1.6$ eV) and acceptor ($E_{opt} \approx 1.9$ eV) counterparts possess complementary absorption across the UV-vis spectrum ($\lambda = 300$–$800$ nm), and yield high short-circuit current densities ($J_{SC}$) of about 8.4 mA cm$^{-2}$ and some of the best open-circuit voltage ($V_{OC}$) figures (ca. 1.1 V) reported to date for BHJ solar cells. Considering the high synthetic modularity of thiophene, adequately substituted all-thiophene polymer acceptors pave the way to a broader class of systems with tunable electronic and optical spectra for efficient all-polymer BHJ solar cells.

The PTPD[2F]T polymers with various branched-alkyl side chains shown in Figure 1 a [2-decyltetradecyl (2DT), 2-octyldodecyl (2OD), 2-hexyldecyl (2HD)] were synthesized by microwave-assisted Stille cross-coupling polymerization (see synthetic methods in the Supporting Information) to control polymer growth and molecular weight (MW), while minimizing reaction times. Side-chain effects have been shown to correlate with material performance in BHJ solar cells with several polymer donors,[13c] and those effects should be accounted for in polymer acceptor designs.[6b,15] The PTPD[2F]T analogues were purified by established protocols:[13c] using the strongly complexing ligand *N*,*N*-diethyl-2-phenyldiazenecarbothioamide to remove palladium residues, and subjecting the polymers to Soxhlet extractions (methanol, dichloromethane) to remove short-chain oligomers, thus affording batches of comparable number-average MW (16.2–18.6 kDa) and polydispersity indexes (PDI = 1.8–2.0; see Table S1 in the Supporting Information). MW effects have been shown to impact charge transport and polymer efficiency in BHJ solar cells.[16] Here, we note that a total of six batches of the PTPD[2F]T(2HD) were prepared to demon-

[*] Dr. S. Liu,[+] Dr. Z. Kan,[+] Dr. S. Thomas, F. Cruciani, Prof. J.-L. Brédas, Prof. P. M. Beaujuge
Physical Science and Engineering Division, Solar & Photovoltaics Engineering Research Center (SPERC), King Abdullah University of Science and Technology (KAUST), Thuwal 23955-6900 (Saudi Arabia)
E-mail: pierre.beaujuge@kaust.edu.sa
[+] These authors contributed equally to this work.

Supporting information for this article can be found under: http://dx.doi.org/10.1002/anie.201604307.

  

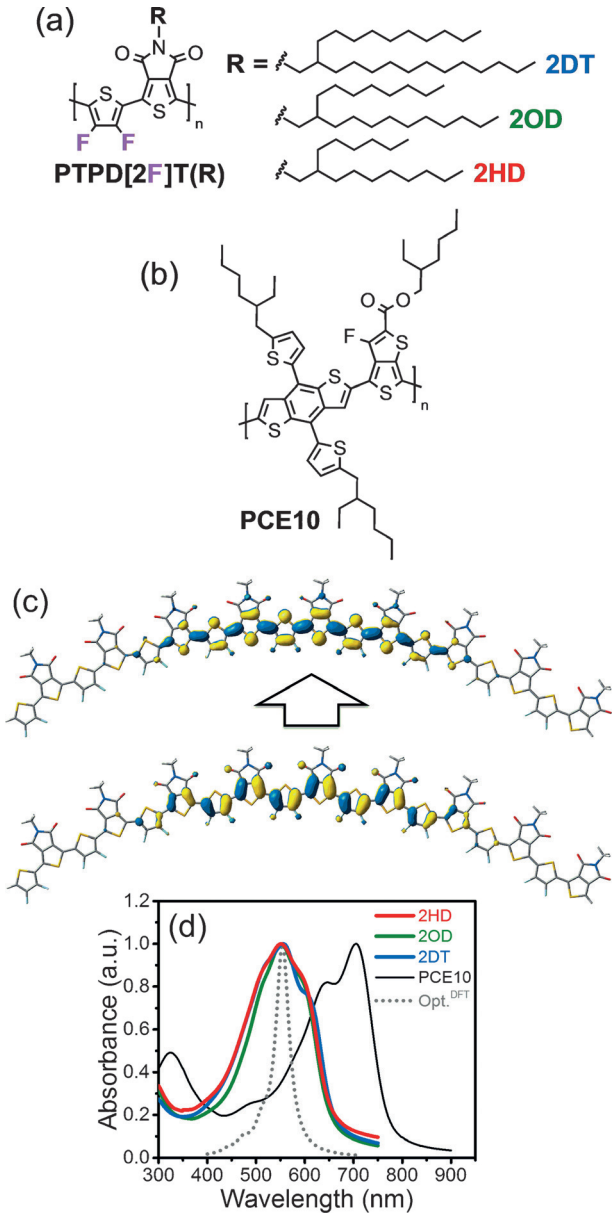


***Figure 1.*** Chemical structures of a) PTPD[2F]T with various branched substituents (2DT, 2OD, 2HD) and b) PCE10 (model system). c) Representations of the TD-DFT tuned-ωB97X-D natural transition orbitals with the largest contribution to the $S_0$–$S_1$ transition for a TPD[2F]T nonamer (bottom: hole wavefunction; top: electron wavefunction). d) Superimposed thin-film UV-vis optical absorption spectra of PTPD-[2F]T and the polymer donor PCE10 (normalized). The dotted curve depicts the tuned-ωB97XD simulated (Gaussian-broadened) optical spectrum of a TPD[2F]T nonamer.

strate batch-to-batch repeatability (see Table S1) and consistency across our device analyses.

Considerations for backbone conformation, π-electron delocalization, and spectral absorption are of particular importance in the design of efficient polymers for BHJ solar cells.[2a] Density functional theory (DFT) modeling is a useful tool in probing those effects and anticipating possible steric hindrance as substituted thiophene motifs—here TPD and [2F]T—are combined within the same backbone.[17] In Figure S4, the potential-energy-surface (PES) plots obtained by incremental rotation of the [2F]T unit relative to the TPD motif shows two minima, corresponding to the 40° and fully planar *anti*/180° conformations, respectively (for details see the Supporting Information). In PTPD[2F]T, *anti* conformations are predicted to be significantly more stable (by 2.0 kcal mol$^{-1}$), and energetic barriers of about 3.8 kcal mol$^{-1}$ are expected to impede interconversion between *syn* and *anti* conformers at room temperature (thermal energy at 300 K = 0.6 kcal mol$^{-1}$). Figure 1c depicts the time-dependent (TD) DFT tuned-ωB97XD natural transition orbitals with the largest contribution to the $S_0$–$S_1$ transition for a TPD[2F]T nonamer, and π-electron delocalization occurs over approximately four repeat units (see the Supporting Information).

The normalized thin-film UV-vis absorption spectra of the PTPD[2F]T polymers and that of the polymer donor PCE10 (model system later used in the BHJ solar cell device study) are superimposed in Figure 1d, and temperature-dependent solution UV-vis spectra are provided in Figures S7 and S8. Figure 1d indicates that the PTPD[2F]T polymers with various branched side chains have near-identical absorption spectra across the range $\lambda = 350$–$650$ nm (peaking at ca. $\lambda =$ 550 nm) and equivalent optical band gaps ($E_{opt} \approx 1.9$ eV). The DFT-simulated optical spectrum for the TPD[2F]T nonamer peaks at $\lambda = 554$ nm. In comparison, the thin-film absorption spectrum of PCE10 extends into the range $\lambda = 425$–$800$ nm, thus showing significant spectral complementarity between $\lambda = 620$ and 800 nm (a critically important aspect in the optimization of BHJ solar cell efficiency). The ionization potentials (IPs) of the PTPD[2F]T polymers were determined to be greater than 5.8 eV by photoelectron spectroscopy in air (PESA; vs. ≈5.0 eV for PCE10; see Figure S9 and Table S3). Expectedly, the large IP values are comparable to those commonly inferred for fullerene acceptors (≈5.9 eV for $PC_{71}BM$ by PESA). Figure S10 shows the oxidation and reduction scans from which the electrochemically-estimated IPs and electron affinities (EAs) were inferred: about 6.3 eV (vs. ≈5.7 eV for PCE10) and 3.8 eV (vs. ≈3.5 eV for PCE10), respectively (see Table S4). EA values are 0.2–0.3 eV lower than those of common fullerene acceptors such as $PC_{61}BM$ and $PC_{71}BM$ (4.1–4.3 eV), and also lower than those of PDI/NDI-based polymer acceptors.[4–6] From these estimates, we note that the lower EA values should be amenable to high $V_{OC}$ in BHJ solar cells.

Thin-film BHJ solar cells with the inverted device architecture ITO/ZnO/PCE10:PTPD[2F]T/$MoO_3$/Ag (device area: 0.1 cm$^2$) were fabricated and tested under AM1.5G solar illumination (100 mW cm$^{-2}$). The cells with optimized PCE10:PTPD[2F]T blend ratios (1:2, wt/wt) were cast from hot 1,2-dichlorobenzene (DCB; ca. 115 °C) on substrates preheated to about 125 °C (see the Supporting Information; film thicknesses in the range 80–90 nm). As shown in Figure 2a and Table 1, optimized BHJ devices made with PCE10 and the PTPD[2F]T polymers with various appended substituents (2DT, 2OD and 2HD) achieved very distinct efficiency patterns. The device statistics, including standard deviations, are provided in Figure S11 and Table S5. While optimized BHJ devices made with the most soluble derivative PTPD[2F]T(2DT) reach only modest $J_{SC}$ and fill-

  

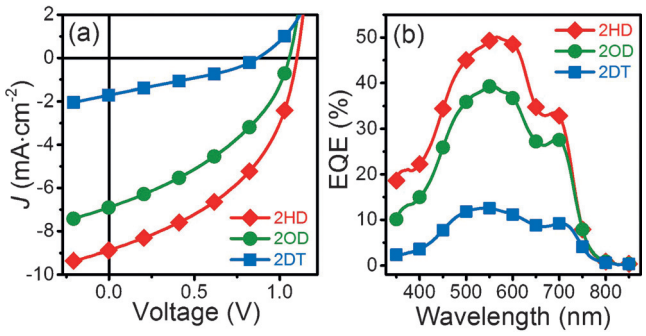


***Figure 2.*** a) Characteristic *J-V* curves and b) EQE spectra of optimized BHJ solar cells fabricated with the polymer donor PCE10 (model system) and the PTPD[2F]T polymer acceptors. AM1.5G solar illumination (100 mW cm$^{-2}$).

***Table 1:*** PV Performance of the PTPD[2F]T derivatives in inverted BHJ devices with PCE10.[a,b]

| Polymer acceptor | $J_{sc}$ [mA cm$^{-2}$] | $V_{OC}$ [V] | FF [%] | Avg. PCE [%] | Max. PCE [%] |
|---|---|---|---|---|---|
| 2DT | 2.1 | 0.8 | 29.9 | 0.5 | 0.7 |
| 2OD | 6.5 | 1.0 | 36.9 | 2.4 | 2.9 |
| 2HD | 8.4 | 1.1 | 44.4 | 4.1 | 4.4 |

[a] Average values across more than 10 devices. [b] Device statistics in Figure S11.

factor (*FF*) values of about 2.1 mA cm$^{-2}$ and 29.9%, respectively, the less bulky branched analogue PTPD[2F]T(2OD) yields a substantially higher $J_{SC}$ value of about 6.5 mA cm$^{-2}$, and concurrently improved *FF* (36.9%) and $V_{OC}$ (ca. 1.0 V). Overall, PTPD[2F]T(2OD)-based devices achieve about a fivefold PCE improvement, reaching up to 2.9% (avg. 2.4%) following the same film-casting conditions. It is interesting to note that, in spite of their rigid-planar backbone conformations (discussed in earlier sections, and depicted in Figure 1c), PTPD[2F]T polymers show adequate solubility in common organic solvents [$CHCl_3$, chlorobenzene (CB), 1,2-dichlorobenzene (DCB)]. Turning to the shorter-chain derivative PTPD[2F]T(2HD), optimized BHJ devices show further improved figures of merit, combining a high $J_{SC}$ value of about 8.4 mA cm$^{-2}$, a slightly larger $V_{OC}$ value (ca. 1.1 V), and a significantly increased *FF* nearing 44.4%. As a result, PTPD[2F]T(2HD)-based devices outperform their counterparts made with PTPD[2F]T(2OD) and PTPD[2F]T(2DT), thus achieving up to 4.4% (avg. 4.1%) in a stark sevenfold PCE improvement over devices made with the longer-chain analogue PTPD[2F]T(2DT). The $V_{OC}$ of 1.1 V, consistent with the reduced EAs estimated for PTPD[2F]T, compared to PCBM (see Table S4), represents one of the highest reported to date for BHJ solar cells with fullerene[18] and nonfullerene acceptors.[4–6] In parallel, the photon energy loss ($E_{loss}$)[19] of 0.5 eV (with $E_{loss} = E_{opt}{}^{min} - eV_{OC}$, and $E_{opt}{}^{min}$ the smallest band gap of either donor and acceptor) is one of the lowest reported values for all-polymer BHJ solar cells,[4–6] noting that $E_{loss}$ values of less than or equal to 0.5 eV are especially difficult to achieve in fullerene-based BHJ devices.[19]

The large differences in $J_{SC}$ values achieved in BHJ solar cells with the various branched-alkyl-substituted PTPD[2F]T polymer acceptors (Table 1) are reflected in the *J-V* curves provided in Figure 2a, and consistent with the external quantum efficiency (EQE) spectra shown in Figure 2b (± 0.5 mA cm$^{-2}$; ± 5%). PTPD[2F]T(2HD)-based BHJ devices have the most prominent spectral response in the $\lambda = 350$–750 nm range, thus showing EQE values reaching about 50% at $\lambda = 550$ nm (abs. max. of PTPD[2F]T; EQE > 40% in the range $\lambda = 475$–625 nm). In comparison, PTPD[2F]T(2DT)-based devices afford less than 15% EQE across the visible spectrum, thus confirming the critical effect of the side-chain pattern on material and BHJ solar cell performance.

To examine the potential contributions of morphological effects to the distinct EQE and device efficiency characteristics obtained for the various branched-alkyl-substituted PTPD[2F]T polymer acceptors, we turned to an examination of the aggregation patterns of the polymers by atomic-force microscopy (AFM; see details and notes on TEM analyses in the Supporting Information). The AFM topography and phase images provided in Figure 3 shows various extents of

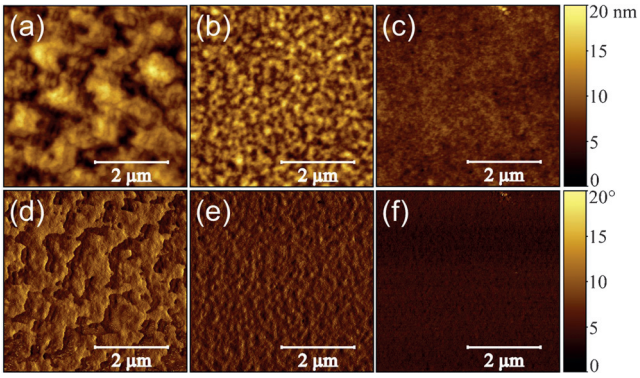


***Figure 3.*** AFM topography (a–c) and phase (d–f) images (tapping mode) for optimized BHJ active layers composed of PCE10 and the PTPD[2F]T polymer acceptors (a,d: 2HD, b,e: 2OD, and c,f: 2DT). Root mean square (RMS) roughness: 2HD, 8.2 nm; 2OD, 2.5 nm; 2DT, 0.6 nm.

aggregation and indicate that the PTPD[2F]T polymers with distinct substituents do not form identical active-layer morphologies with PCE10. In particular, the coarser aggregation pattern observed for PTPD[2F]T(2HD) (RMS roughness: 8.2 nm) contrasts with that for PTPD[2F]T(2DT) (RMS roughness: 0.6 nm), and may correlate with a more pronounced, favorable degree of phase separation between polymer donor and acceptor (a detailed morphology study is beyond the scope of this concise report). Preliminary X-ray analyses suggest that aggregates formed in the BHJ thin films are disordered (see Figure S14).

Figure 4 and Table 2 summarize the results of our carrier mobility examinations in optimized BHJ thin films (see Figure S15), and indicate that hole ($\mu_h$) and electron ($\mu_e$) mobilities are the most balanced in PTPD[2F]T(2HD)-based BHJ devices, where $\mu_e$ reaches $2.35 \times 10^{-5}$ cm$^2$ V$^{-1}$ s$^{-1}$ [vs. $3.16 \times 10^{-8}$ cm$^2$ V$^{-1}$ s$^{-1}$ for PTPD[2F]T(2DT)].

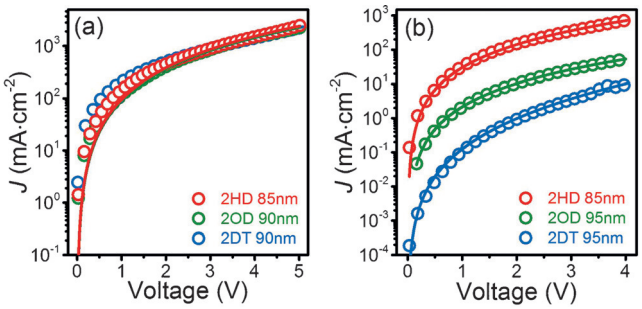


***Figure 4.*** Dark current density-voltage characteristics for a) hole-only (ITO/$MoO_3$/PCE10:PTPD[2F]T/$MoO_3$/Ag) and b) electron-only (ITO/Al/PCE10:PTPD[2F]T/Al) diodes made with optimized BHJ active layers composed of PCE10 and the PTPD[2F]T polymer acceptors (2DT, 2OD, and 2HD).

***Table 2:*** Carrier mobility estimates obtained by space charge-limited current (SCLC) analyses for optimized BHJ thin films with PTPD[2F]T and PCE10.

| Polymer acceptor | $\mu_h$ [$cm^2 V^{-1} s^{-1}$] | $\mu_e$ [$cm^2 V^{-1} s^{-1}$] | $\mu_h/\mu_e$ |
|---|---|---|---|
| 2DT | $2.13\times10^{-4}$ | $3.16\times10^{-8}$ | 6740 |
| 2OD | $1.81\times10^{-4}$ | $4.30\times10^{-6}$ | 42 |
| 2HD | $1.96\times10^{-4}$ | $2.35\times10^{-5}$ | 8 |

In summary, we show that branched-alkyl-substituted PTPD[2F]T polymers can be used as fullerene alternatives in BHJ solar cells, thus achieving some of the best $V_{OC}$ figures (ca. 1.1 V) reported to date for BHJ devices, and PCEs of up to 4.4% with the polymer donor PCE10 (as model system). Our DFT analyses indicate that PTPD[2F]T backbones are expected to be rigid-planar, with main-chain conformations dominantly *anti* and well delocalized frontier orbitals. In PTPD[2F]T-based BHJ active layers, we find that side-chain-induced morphological effects translate into distinct charge-transport patterns, with the shorter-chain derivative PTPD-[2F]T(2HD) concurrently yielding the most balanced carrier mobilities and the best EQE response across the UV-visible spectrum. While, at this time, most efficient polymer acceptors are based on PDI/NDI motifs, adequately substituted all-thiophene polymer acceptors pave the way to a broader class of systems with tunable electronic and optical spectra for further examinations of the all-polymer BHJ concept. The examination of other polymer donors will be of importance in future work with PTPD[2F]T polymers.

## Acknowledgements

The authors acknowledge financial support under Baseline Research Funding from King Abdullah University of Science and Technology (KAUST) and from ONR-Global (Award N62909-15-1-2003 to JLB). The authors thank M. Neophytou for some contributions in the early project developments, R.-Z. Liang for the morphology characterizations by TEM, and P. Wucher for the melting point examinations by DSC.

**Keywords:** density-functional calculations · electron microscopy · materials science · polymers · solar cells

**How to cite:** *Angew. Chem. Int. Ed.* **2016**, *55*, 12996–13000
*Angew. Chem.* **2016**, *128*, 13190–13194

[1] J. J. M. Halls, C. A. Walsh, N. C. Greenham, E. A. Marseglia, R. H. Friend, S. C. Moratti, A. B. Holmes, *Nature* **1995**, *376*, 498–500.
[2] a) P. M. Beaujuge, J. M. J. Fréchet, *J. Am. Chem. Soc.* **2011**, *133*, 20009–20029; b) A. Facchetti, *Mater. Today* **2013**, *16*, 123–132; c) H. Benten, D. Mori, H. Ohkita, S. Ito, *J. Mater. Chem. A* **2016**, *4*, 5340–5365.
[3] a) J. Zhao, Y. Li, G. Yang, K. Jiang, H. Lin, H. Ade, W. Ma, H. Yan, *Nat. Energy* **2016**, *1*, 15027; b) Z. Wu, C. Sun, S. Dong, X. Jiang, S. Wu, H. Wu, H. Yip, F. Huang, Y. Cao, *J. Am. Chem. Soc.* **2016**, *138*, 2004–2013.
[4] T. Kim, J.-H. Kim, T. E. Kang, C. Lee, H. Kang, M. Shin, C. Wang, B. Ma, U. Jeong, T.-S. Kim, B. J. Kim, *Nat. Commun.* **2015**, *6*, 8547.
[5] a) E. Zhou, J. Cong, Q. Wei, K. Tajima, C. Yang, K. Hashimoto, *Angew. Chem. Int. Ed.* **2011**, *50*, 2799–2803; *Angew. Chem.* **2011**, *123*, 2851–2855; b) Y. Zhou et al., *Adv. Mater.* **2014**, *26*, 3767–3722; c) S. Li, H. Zhang, W. Zhao, L. Ye, H. Yao, B. Yang, S. Zhang, J. Hou, *Adv. Energy Mater.* **2016**, *6*, 1501991.
[6] a) Y.-J. Hwang, B. A. E. Courtright, A. S. Ferreira, S. H. Tolbert, S. A. Jenekhe, *Adv. Mater.* **2015**, *27*, 4578–4584; b) J. W. Jung, J. W. Jo, C.-C. Chueh, F. Liu, W. H. Jo, T. P. Russell, A. K. Y. Jen, *Adv. Mater.* **2015**, *27*, 3310–3317; c) X. Zhan, Z. Tan, B. Domercq, Z. An, X. Zhang, S. Barlow, Y. Li, D. Zhu, B. Kippelen, S. R. Marder, *J. Am. Chem. Soc.* **2007**, *129*, 7246–7247; d) C. Mu et al., *Adv. Mater.* **2014**, *26*, 7224–7230; e) L. Gao, Z.-G. Zhang, L. Xue, J. Min, J. Zhang, Z. Wei, Y. Li, *Adv. Mater.* **2016**, *28*, 1884–1890; f) L. Gao, Z.-G. Zhang, L. Xue, J. Min, J. Zhang, Z. Wei, Y. Li, *Adv. Mater.* **2016**, *28*, 1884–1890.
[7] W. Li, W. S. C. Roelofs, M. Turbiez, M. M. Wienk, R. A. J. Janssen, *Adv. Mater.* **2014**, *26*, 3304–3309.
[8] C. R. McNeill, A. Abrusci, J. Zaumseil, R. Wilson, M. J. McKiernan, J. H. Burroughes, J. J. M. Halls, N. C. Greenham, R. H. Friend, *Appl. Phys. Lett.* **2007**, *90*, 193506.
[9] R. Stalder, J. Mei, J. Subbiah, C. Grand, L. A. Estrada, F. So, J. R. Reynolds, *Macromolecules* **2011**, *44*, 6303–6310.
[10] R. Zhao, C. Dou, Z. Xie, J. Liu, L. Wang, *Angew. Chem. Int. Ed.* **2016**, *55*, 5313–5317; *Angew. Chem.* **2016**, *128*, 5399–5403.
[11] T. W. Holcombe, C. H. Woo, D. F. J. Kavulak, B. C. Thompson, J. M. J. Fréchet, *J. Am. Chem. Soc.* **2009**, *131*, 14160–14161.
[12] C. B. Nielsen, S. Holliday, H.-Y. Chen, S. J. Cryer, I. McCulloch, *Acc. Chem. Res.* **2015**, *48*, 2803–2812.
[13] a) A. Pron, P. Berrouard, M. Leclerc, *Macromol. Chem. Phys.* **2013**, *214*, 7–16; b) X. Guo, A. Facchetti, T. J. Marks, *Chem. Rev.* **2014**, *114*, 8943–9021; c) C. Cabanetos, A. El Labban, J. A. Bartelt, J. D. Douglas, W. R. Mateker, J. M. J. Frechet, M. D. McGehee, P. M. Beaujuge, *J. Am. Chem. Soc.* **2013**, *135*, 4656–4659.
[14] a) J. Wolf, F. Cruciani, A. El Labban, P. M. Beaujuge, *Chem. Mater.* **2015**, *27*, 4184–4187; b) C. J. Mueller, C. R. Singh, M. Fried, S. Huettner, M. Thelakkat, *Adv. Funct. Mater.* **2015**, *25*, 2725–2736.
[15] C. Lee, H. Kang, W. Lee, T. Kim, K.-H. Kim, H. Y. Woo, C. Wang, B. J. Kim, *Adv. Mater.* **2015**, *27*, 2466–2471.
[16] N. Zhou et al., *J. Am. Chem. Soc.* **2016**, *138*, 1240–1251.
[17] a) M. J. Frisch, et al., Gaussian, Inc.: Wallingford, CT, USA, **2009**; b) T. Stein, L. Kronik, R. Baer, *J. Am. Chem. Soc.* **2009**, *131*, 2818–2820; c) T. Körzdörfer, J.-L. Brédas, *Acc. Chem. Res.* **2014**, *47*, 3284–3291.

  

[18] S.-H. Liao, H.-J. Jhuo, Y.-S. Cheng, S.-A. Chen, *Adv. Mater.* **2013**, *25*, 4766 – 4771; H.-J. Jhuo, Y.-S. Cheng, S.-A. Chen, *Adv. Mater.* **2013**, *25*, 4766 – 4771.

[19] a) W. Li, K. H. Hendriks, A. Furlan, M. M. Wienk, R. A. J. Janssen, *J. Am. Chem. Soc.* **2015**, *137*, 2231 – 2234; b) M. Wang, H. Wang, T. Yokoyama, X. Liu, Y. Huang, Y. Zhang, T.-Q. Nguyen, S. Aramaki, G. C. Bazan, *J. Am. Chem. Soc.* **2014**, *136*, 12576 – 12579; c) K. Kawashima, Y. Tamai, H. Ohkita, I. Osaka, K. Takimiya, *Nat. Commun.* **2015**, *6*, 10085.

Received: May 3, 2016
Revised: July 22, 2016
Published online: September 16, 2016

  